Supplementary Information (SI) for Journal of Materials Chemistry C.

Electronic Structure Engineering in NiFe Layered double hydroxide via A first row transition metals doping as an Efficient Electrochemical oxidation performance of Sulfamethazine in food samples

Francis Packiaraj Don Disouza [a1], Antony Jasmine Vincent John [a1], Shen-Ming Chen[a,] *, Hung Cheng Yu [a]

[a]Department of Chemical Engineering and Biotechnology, National Taipei University of Technology, No. 1, Section 3, Chung-Hsiao East Road, Taipei 106, Taiwan.

[1] Authors contributed equally to this work.

* Corresponding author: Chen, S.M (smchen1957@gmail.com)

Chemicals and Reagents

Titanium dioxide (TiO_2, ReagentPlus , ≥99%), Sodium metavanadate ($NaVO_3$, anhydrous grade, 99.9% trace metals basis), Chromium(III) chloride hexahydrate ($CrCl_3 \cdot 6H_2O$, 96%, solid), Manganese(II) chloride tetrahydrate, ($MnCl_2 \cdot 4H_2O$, ReagentPlus ≥99%), Iron(III) chloride hexahydrate ($FeCl_3 \cdot 6H_2O$, ACS reagent, 97%), Cobalt(II) chloride hexahydrate, ($CoCl_2 \cdot 6H_2O$, ACS reagent, 98%), Nickel (II) chloride hexahydrate, ($NiCl_2 \cdot 6H_2O$, 99.999% trace metals basis), Copper(II) chloride dihydrate ($CuCl_2 \cdot 2H_2O$, ACS reagent, ≥99.0%), zinc chloride, ($ZnCl_2$, Reagent grade, ≥98%), Sulfamethazine (purity 99.0–101.0 %), all chemicals were obtained from Sigma-Aldrich and utilized directly without any additional purification.

Electrode Fabrication

To prepare the graphitic carbon electrode (GCE), its surface was polished with alumina slurry and subsequently rinsed with deionized water and anhydrous ethanol. The catalyst suspension was prepared by dispersing 3 mg of NiFeSc-LD, NiFeTi-LDH, NiFeV-LDH, NiFeCr-LDH, NiFeMn-LDH, NiFeCo-LDH, and NiFeCu-LDH and NiFeZn-LDH in 1 mL of deionized water, followed by ultrasonic treatment in a water bath for 6 hours to ensure uniform distribution. Then, 6 μL of the resulting suspension was drop-cast onto the GCE surface and dried in a conventional oven at 60 °C for 10 minutes.

Physical characterization

The structural characterization of the synthesized electrocatalyst was conducted using the X'Pert3 Powder X-ray diffractometer (Malvern Panalytical, UK). The Thermo ESCLAB 250

instrument was used for X-ray photoelectron spectroscopy (XPS). Morphology of the electrocatalyst was examined using field emission scanning electron microscopy (FE-SEM) (JEOL JSM-6500F, Akishima, Tokyo, Japan) and high-resolution transmission electron microscopy (HR-TEM: JEM 2100 F, JEOL Ltd., Japan), accompanied by energy dispersive X-ray spectroscopy (EDX). For electrochemical analysis, a three-electrode configuration was used; consequently, a Pt wire was used as the counter electrode, an Ag/AgCl in saturated KCl was utilized as a reference electrode, and the glassy carbon electrode (GCE) was used as the working electrode. The electrical resistivity of the materials was measured using an EIS-IM6ex ZAHNER, and the data were analyzed with a ZAHNER analyzer in 5 mM $[Fe(CN)_6]^{3-/4-}$ with 0.1 M KCl as the electrolyte. The EIS measurement was performed over a frequency range of 0.1 Hz to 10,000 Hz with a 5 mV amplitude. Cyclic voltammetry (CV) was conducted using a CHI 1205 B instrument, and Different Pulse Voltammetry (DPV) electrochemical equivalents were made on the CHI 900 within the potential range of 0.0-1.2 V in 0.1 M PBS (pH 7).

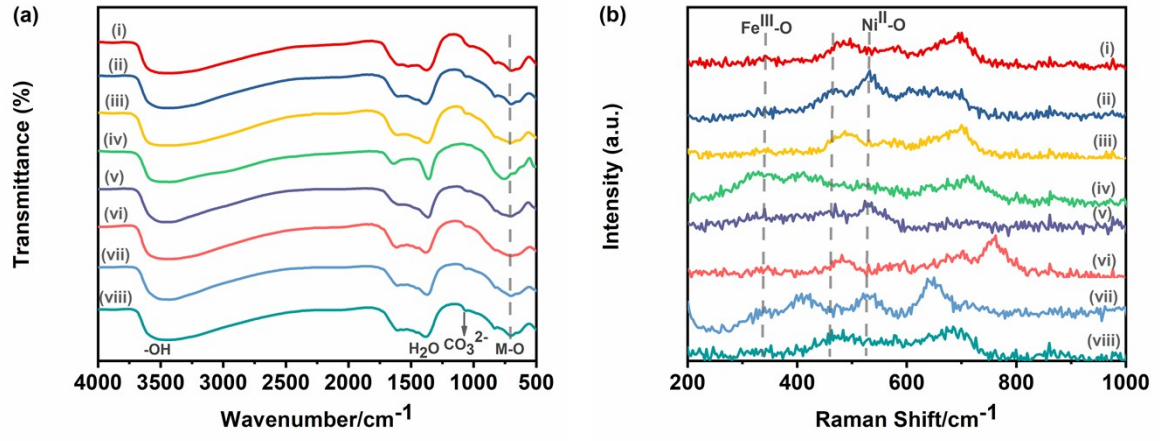

Fig. S1. (a-b) FT-IR and Raman spectra of (i) NiFeZn-LDH, (ii) NiFeCu-LDH, (iii) NiFeCo-LDH, (iv) NiFeMn-LDH, (v) NiFeCr-LDH, (vi) NiFeV-LDH, (vii) NiFeTi-LDH, (viii) NiFe-LDH, respectively.

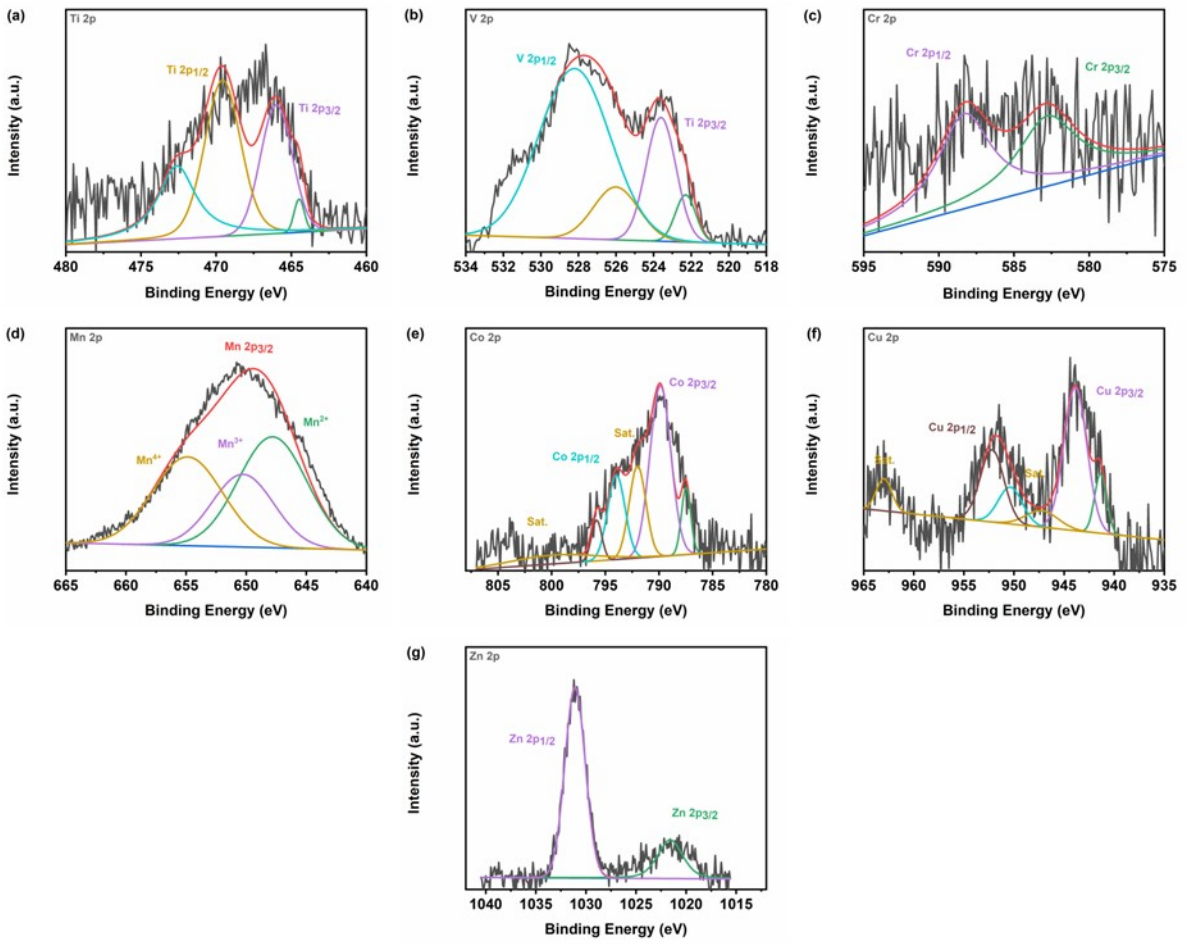

Fig. S2. XPS (a) Ti 2p, (b) V 2p, (c) Cr 2p, (d) Mn 2p, (e) Co 2p, (f) Cu 2p, and (g) Zn 2p spectra of NiFeTi-LDH, NiFeV-LDH, NiFeCr-LDH, NiFeMn-LDH, NiFeCo-LDH, NiFeCu-LDH, and NiFeZn-LDH, respectively.

The Ti 2p XPS spectrum displays peaks at 464.5 eV (Ti $2p_{3/2}$) and 469.5 eV (Ti $2p_{1/2}$), which are attributed to Ti^{3+}, whereas the peaks near 466 eV (Ti $2p_{3/2}$) and 472.7 eV (Ti $2p_{1/2}$) correspond to Ti^{4+} [1]. In the V 2p region, the peaks at 522.3 eV (V $2p_{3/2}$) and 526 eV (V $2p_{1/2}$) indicate the presence of V^{5+}, while those at 523.6 eV (V $2p_{3/2}$) and 528.2 eV (V $2p_{3/2}$) are assigned to V^{5+} [2]. The Mn $2p_{3/2}$ spectrum exhibits three characteristic peaks at approximately 647.8, 650.4, and 655 eV, corresponding to Mn^{2+}, Mn^{3+}, and Mn^{4+}, respectively [3]. For chromium, the Cr 2p signals at 582.7 eV (Cr $2p_{3/2}$) and 588.2 eV (Cr $2p_{1/2}$) are associated with Cr^{3+} [4]. The Co 2p spectrum features peaks at 787.5 and 789.9 eV assigned to Co^{3+} and Co^{2+}

species in the Co $2p_{3/2}$ region, respectively, along with peaks at 793.9 and 795.8 eV corresponding to Co^{3+} and Co^{2+} in the Co $2p_{1/2}$region, along with the satellite peak at 792 and 800.5 eV [5]. The Cu 2p spectrum shows peaks at 941.4 eV (Cu $2p_{3/2}$) and 950.4 eV (Cu $2p_{1/2}$), indicative of Cu^{+}, whereas the peaks around 943.9 eV (Cu $2p_{3/2}$) and 952.2 eV (Cu $2p_{1/2}$) are characteristic of Cu^{2+} [6]. The Zn 2p spectra at 1021.6 eV (Zn $2p_{3/2}$) and 1031.1 eV (Zn $2p_{1/2}$) are associated with Zn^{2+} [7].

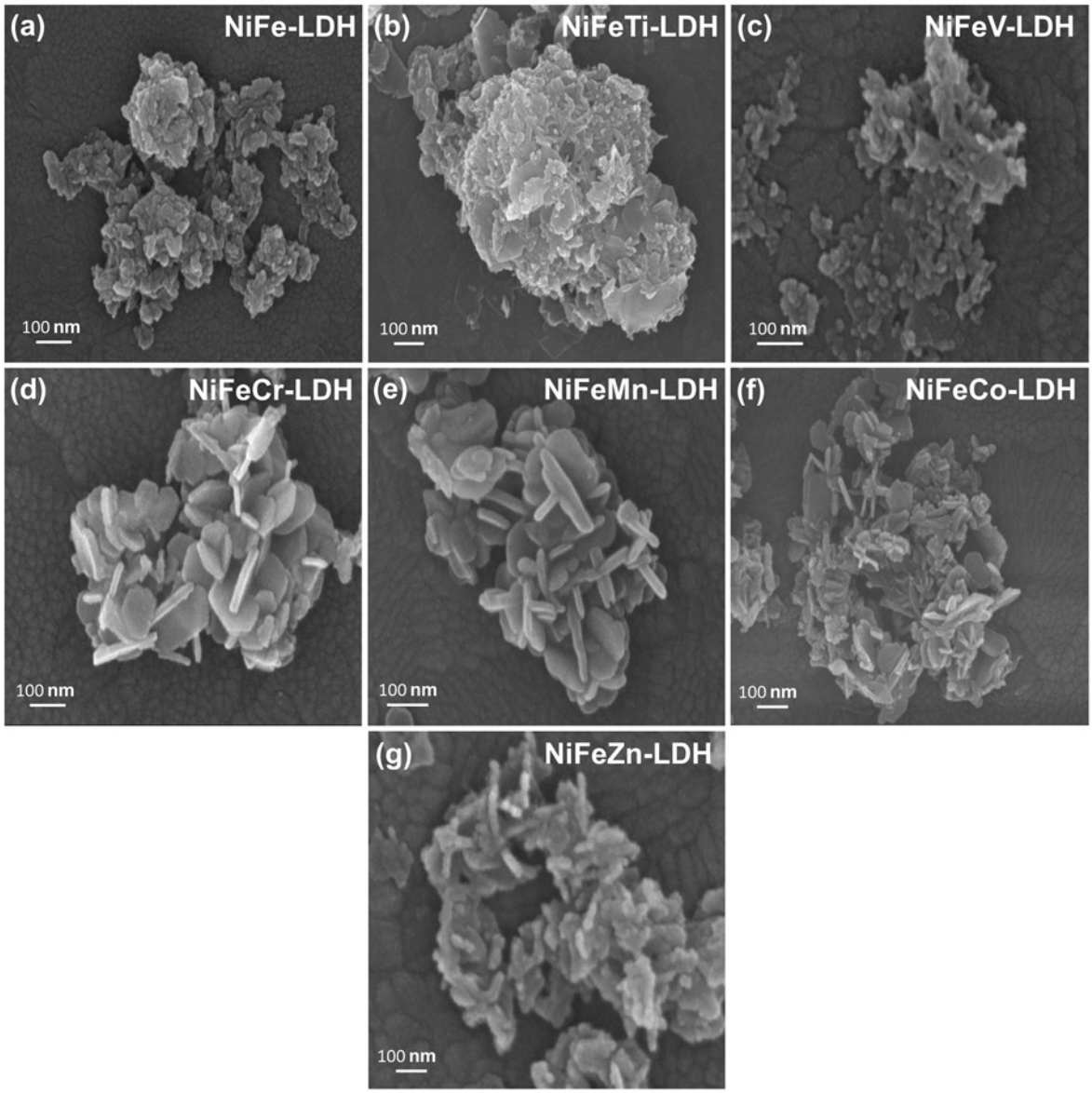

Fig. S3. FE-SEM image of (a) NiFe-LDH, (b) NiFeTi-LDH/GCE, (c) NiFeV-LDH, (d) NiFeCr-LDH, (e) NiFeMn-LDH, (f) NiFeCo-LDH, and (g) NiFeZn-LDH

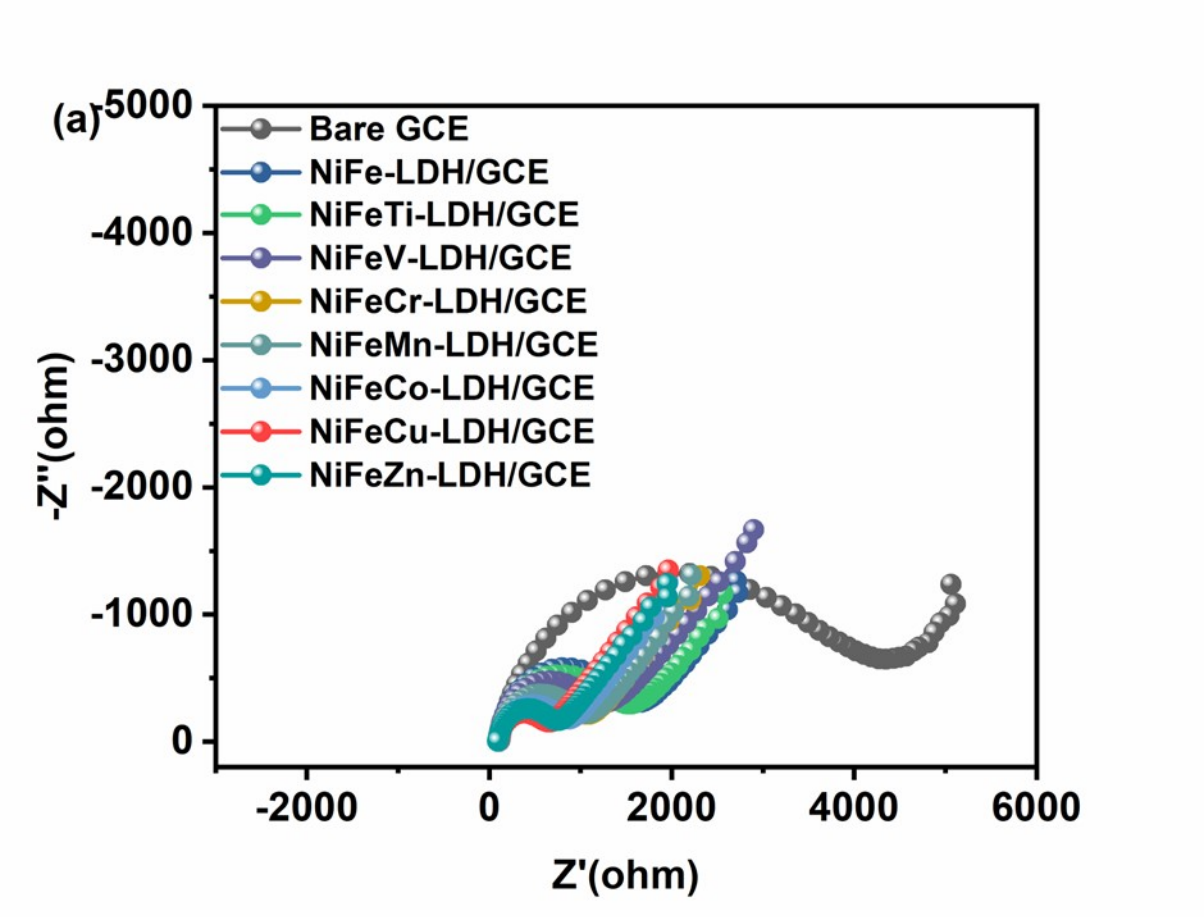

Fig. S4. (a) EIS spectra of Bare GCE, NiFe-LDH, NiFeTi-LDH/GCE, NiFeV-LDH, NiFeCr-LDH, NiFeMn-LDH, NiFeCo-LDH, NiFeCu-LDH and NiFeZn-LDH.

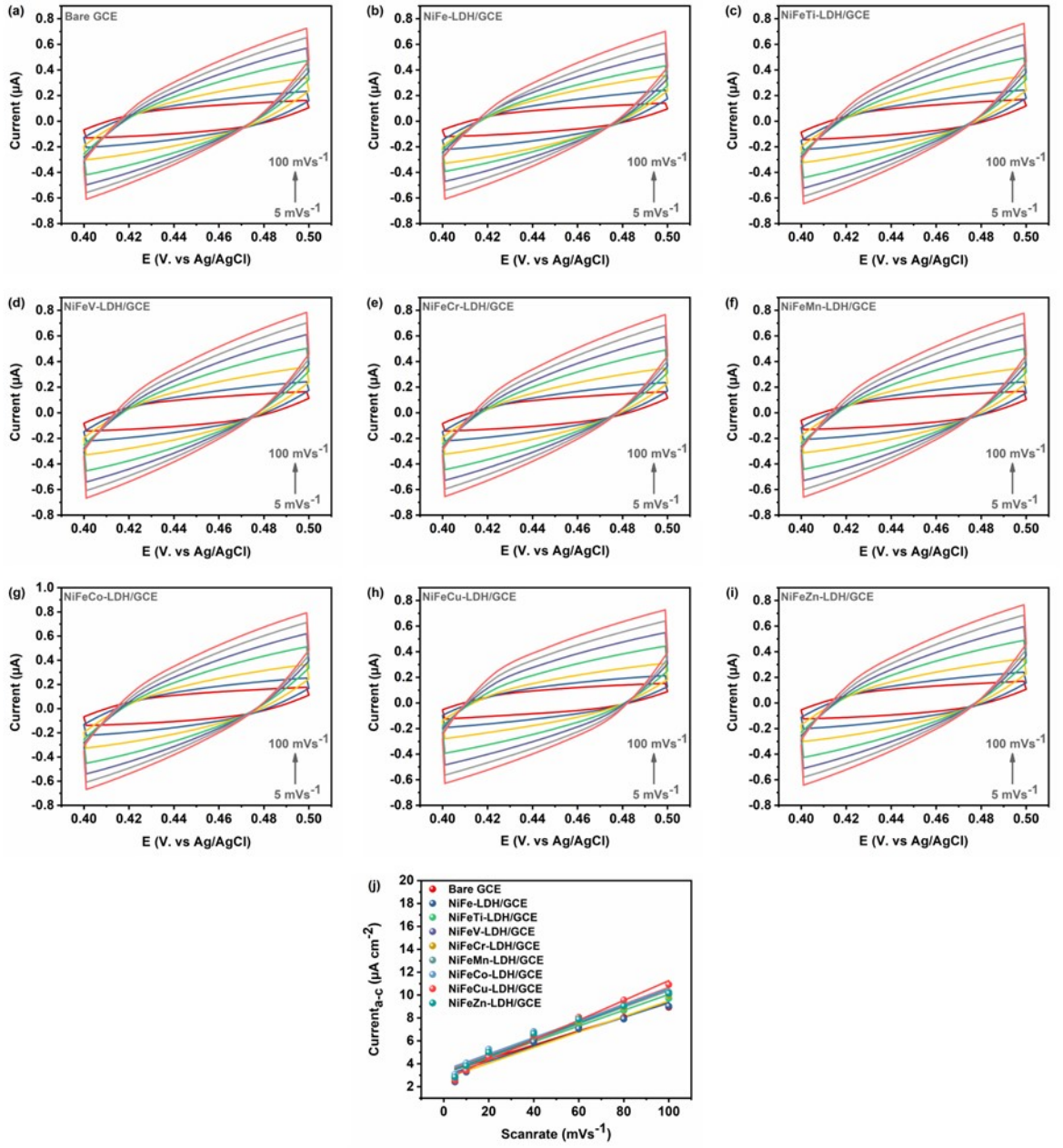

Fig. S5. (a-i) cyclic voltammetry, various scan rate measurements of Bare GCE, NiFe-LDH, NiFeTi-LDH/GCE, NiFeV-LDH, NiFeCr-LDH, NiFeMn-LDH, NiFeCo-LDH, NiFeCu-LDH and NiFeZn-LDH in 0.1 M PBS (pH 7) at 5 to 100 mV s^{-1} in the non-Faradaic region, (j) equivalent linear graph of scan rate vs redox current response of $Current_{a-c}$ (μA cm^{-2}).

Table S1. The comparative ECSA of Bare GCE, NiFe-LDH/GCE, NiFeTi-LDH/GCE, NiFeV-LDH/GCE, NiFeCr-LDH/GCE, NiFeMn-LDH/GCE, NiFeCo-LDH/GCE, NiFeCu-LDH/GCE and NiFeZn-LDH/GCE.

Electrode	**Substrate**	**Double-layer capacitance (cdl) ($\mu F\ cm^{-2}$)**	**Electrochemical active surface area (ECSA) (cm^2)**
Bare	GCE	30.65	2.17
NiFe-LDH	GCE	31.95	2.26
NiFeTi-LDH	GCE	34.55	2.45
NiFeV-LDH	GCE	36.35	2.58
NiFeCr-LDH	GCE	36.15	2.56
NiFeMn-LDH	GCE	36.75	2.60
NiFeCo-LDH	GCE	35.75	2.53
NiFeCu-LDH	GCE	43.25	3.07
NiFeZn-LDH	GCE	36.95	2.62

Reference

[1] D. Gonbeau, C. Guimon, G. P□ ster-Guillouzo, A. Levasseur, G. Meunier and R. Dormoy, Surf. Sci 254 (1991) 81–89.

[2] F.N.I. Sari, H.-S. Chen, A. kumar Anbalagan, Y.-J. Huang, S.-C. Haw, J.-M. Chen, C.-H. Lee, Y.-H. Su, J.-M. Ting, V-doped, divacancy-containing β-FeOOH electrocatalyst for high performance oxygen evolution reaction, Chem. Eng. J. 438 (2022) 135515.

[3] F.N.I. Sari, K.-C. Lin, J.-M. Ting, Mn (OH) 2-containing Co (OH) 2/Ni (OH) 2 Core-shelled structure for ultrahigh energy density asymmetric supercapacitor, Appl. Surf. Sci. 576 (2022) 151805.

[4] S. Li, T.X. Nguyen, Y. Su, C. Lin, Y. Huang, Y. Shen, C. Liu, J. Ruan, K. Chang, J. Ting, Sputter-deposited high entropy alloy thin film electrocatalyst for enhanced oxygen evolution reaction performance, Small 18 (2022) 2106127.

[5] F.N.I. Sari, N.T.T. Tran, Y.-X. Lin, S.-Y. Li, Y.-H. Shen, J.-M. Ting, Electronic structure modification induced electrochemical performance enhancement of bi-functional multi-metal hydroxide, Electrochim. Acta 439 (2023) 141616.

[6] F.N.I. Sari, B.W. Saputro, J.-M. Ting, Structural and defect modulations of co-precipitation synthesized high-entropy Prussian blue analogue nanocubes via Cu/Zn co-doping for enhanced electrochemical performance, J. Mater. Chem. A 11 (2023) 19483–19495.

[7] D. Xu, D. Fan, W. Shen, Catalyst-free direct vapor-phase growth of Zn1− x Cu x O micro-cross structures and their optical properties, Nanoscale Res. Lett. 8 (2013) 46.